X-ray waveguides with multiple guiding layers

F. Pfeiffer and T. Salditt
Sektion Physik der Ludwig-Maximilians-Universität München, Geschwister-Scholl-Platz 1, 80539 München, Germany

P. Høghøj and I. Anderson
Institut Laue-Langevin, Boîte Postale 156, 38042 Grenoble Cedex 9, France

N. Schell
Forschungszentrum Rossendorf, ROBL (ESRF), P.O. Box 510019, 01314 Dresden, Germany
(Received 25 May 2000)

We have generalized the principle of resonant x-ray beam coupling to waveguides containing multiple guiding layers and characterized their x-ray optical properties. In such a device, several coherent beams of a width on the order of 10–100 nm can be extracted at the end of the waveguide. By measuring the farfield pattern formed by the interference of the beams, we demonstrate the possibility of using these devices as new tools to tailor the field distribution in the near- and far-field region for specific applications. Besides coherent diffraction and imaging, interferometry with two or more nanometer sized beams can be envisioned.

During recent years, several new techniques using coherent x-ray beams have evolved upon the availability of new and highly brilliant synchrotron radiation sources, ranging from coherent diffraction and photon correlation spectroscopy[1–3] to hard x-ray microscopy and imaging.[4] New optical devices for coherent hard x-ray radiation may lead to further improvements. Submicrometer spot sizes of coherent beams have recently been achieved by Fresnel lenses.[5] However, current lithographic processes and an absorption contrast decreasing with photon energy limit the performance of both Fresnel and Bragg-Fresnel-type optics in the regime of hard x-rays. Providing an alternative route, Feng and co-workers proposed the use of x-ray waveguide structures and demonstrated the feasibility of a resonant beam coupling device, which produces a coherent and divergent x-ray beam with precisely defined properties concerning beam shape and coherence.[6] Following this principle, Lagomarsino and co-workers performed a lenseless phase contrast microscopy experiment with submicrometer resolution in one direction. For the demonstration experiment the authors have used a waveguided beam with a cross section of ~1300 Å [full width at half maximum (FWHM)] in a transmission microscopy setup.[7] We have recently shown that even beam widths of less than 100 Å can be achieved by the technique.[8]

The basic structure of a hard x-ray waveguide consists of a low density guiding layer sandwiched in between layers of high density. Accordingly, the guided modes are resonantly excited by shining a parallel beam onto the waveguide under grazing incidence at a set of discrete angles $\alpha_{i,n}$. A coherent beam exits the structure at the side with a cross section corresponding to the thickness of the guiding layer and a divergence given by the FWHM of the Fourier transform of the excited standing wavefield [see also Eq. (1)]. The divergence of the exiting guided mode, the angular acceptance, and the absolute number of supported modes, can be all controlled by the structural and geometric parameters and varied within a certain range.[9,10] However, single guiding layer waveguides are characterized by strong restrictions, concerning particularly the shape in the nearfield and thus in the farfield pattern. Additionally, high coupling efficiencies of single guiding layer waveguides can only be achieved for a very small angular acceptance of the incident beam (typically a few thousandths of a degree).[11] A broader angular acceptance combined with a more divergent x-ray source would lead to an increased absolute flux throughput compared to the performance of a conventional waveguide at such a source. In order to overcome these limitations, we have generalized the concept of resonant beam coupling devices (x-ray waveguides) in the present work from single to multiple guiding layers. By multiple guiding layer waveguides one can generate more complex and specifically tailored field distributions in the near- and far-field regions. Most importantly, this scheme may open a new way to perform x-ray holography and interferometry experiments using two or more coherent beams of nanometer dimensions.

Figure 1 shows the schematic of a waveguide structure consisting of several guiding layers of a low density material (such as carbon) with an index of refraction n_1 and a thickness d_1 separated by comparably thin layers of a high density material (such as nickel) with d_2 and n_2, respectively. Towards the substrate (silicon or floatglass) the periodic multilayer structure is bounded by a thick bottom layer (thickness d_b, index n_2). To gain an understanding of the mode excitation and waveguide properties, we have calculated the internal (and external) standing electromagnetic field as a function of the structural and geometric parameters (layer thickness, composition and density, interface roughness, angles of incidence, x-ray energy) by a transfer matrix algorithm similar to the one used in the case of optical waveguides.[12] Equivalently, one can use the well known Parratt formalism[13] for such calculations. The results can be conveniently illustrated by two-dimensional contour plots, where the field amplitude or intensity is shown as a function of the incidence angle α_i and depth into the sample z. In Fig. 2 calculations for waveguides with one (top), two (middle), and multiple (bottom) guiding layers are shown, with the

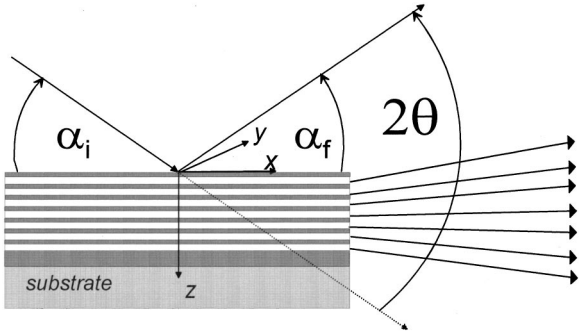

FIG. 1. Sketch of a multiple guiding layer waveguide with exiting beams interfering at the side of the sample.

electric field intensity $|E_y(z)|^2$ coded in a logarithmically scaled table of gray shades (black corresponds to a high field intensity).

In the simplest case with only one guiding layer (top) mode excitation appears for a set of nearly discrete values of α_i in a range between the critical angle of the guiding layer $\alpha_{c1}=\sqrt{2\delta_1}\sim 0.081°$ and $\alpha_{c2}=\sqrt{2\delta_2}\sim 0.171°$ (separation layers/bottom layer, 20 keV x-rays).[14] The angular acceptance of the TE0 (zero-order transverse electric) mode in such a structure is typically of the order of several thousandths of a degree. The enhancement of the electric field intensity respective to the incident beam reaches a factor of $\sim$120 for $\alpha_{i,\mathrm{TE0}}$. Note also that absorption was included in these calculations, although it turned out to have only a minor effect for x-ray energies of $\lambda<1$ Å. Equally, interfacial roughness did not significantly alter the intensity values since the product of the rms roughness σ and the internal wave vectors k_z' remained small, as long as σ did not exceed 15 Å by far.

Adding another guiding layer (Fig. 2, middle) leads to a splitting of the single modes into submodes with a symmetric (at smaller α_i) and antisymmetric phase shape (greater α_i), analogous to the quantum mechanical tunnel splitting in double well potentials or overlapping *s* orbitals in quantum chemistry. Thus we are able to produce a resonantly enhanced internal field distribution with a shape similar to the TE1 mode of a single-layer guide, but with a different phase pattern. Another important point is the increased angular acceptance, i.e., ''allowed'' angles of incidence, for which mode excitation inside the guide appears. Additionally there is no loss in the maximum field enhancement, as would result, e.g., from a simple decrease in the top layer thickness of a single-layer guide. A further increase in the number of guiding layers leads to a set of guiding bands, where mode excitation is observed within intervals of α_i, see Fig. 2 (bottom). Note that the single submodes in the two guiding bands are still discernible. A more detailed analysis shows that the electric field amplitudes and shapes of these submodes depend very sensitively on α_i and very complex phase distributions can be achieved by selecting the corresponding excited submode. In the limit of an infinite number of guiding layers a perfect bandlike behavior results, and it is no longer possible to select a single submode, also because of the dramatically enhanced probability of modemixing in the latter case.

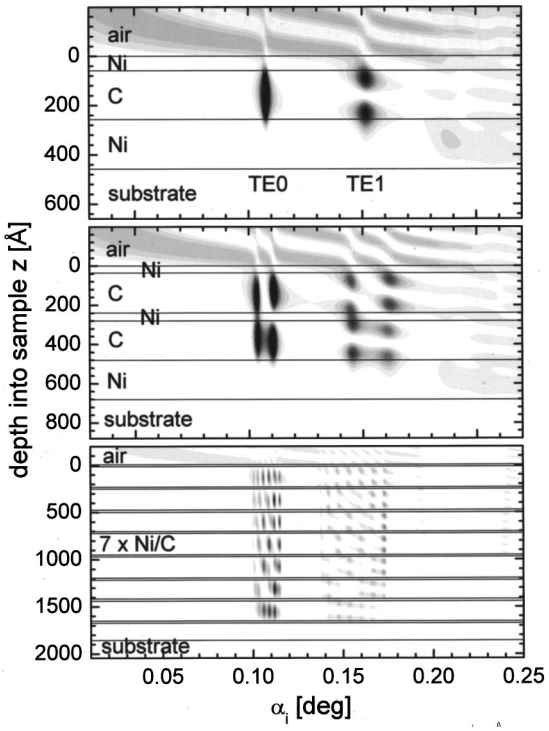

FIG. 2. Contour plots of the calculated electric field intensity $|E_y(z)|^2$ inside Ni/C waveguides with one (top), two (middle), and seven (bottom) guiding layers (20 keV x rays).

To experimentally demonstrate the effects calculated above and to fabricate the first multiple guiding layer structures, a series of differently designed waveguides was fabricated by dc magnetron sputtering. The x-ray experiments were carried out at the bending magnet beamline ROBL of ESRF with a Si[111] double monochromator adjusted to an x-ray energy of 20 keV. We used a beamsize at the sample of 0.1 mm (vert.)×0.1 mm (hor.) and a fast scintillation detector mounted on the detector arm at a distance of 680 mm. In Fig. 3, the measured reflectivity of a single guiding layer structure (55 Å Ni/1098 Å C/220 Å Ni/floatglass-substrate), a waveguide with two guiding layers (75 Å Ni/98 Å C/97 Å Ni/94 Å C/202 Å Ni/substrate) and a multiple guiding layer waveguide (7×[25 Å Ni/457 Å C]/200 Å Ni/floatglass-substrate) are shown. Apart from the above thickness values, an average rms roughness of $\sigma\sim 9$ Å, and an additional oxide layer of a thickness of 14 Å at the top was obtained from a reflectivity fitting procedure based on the film densities of nickel and carbon typically observed in sputtering.

The waveguide effects readily manifest themselves in the reflectivity curve as cusps in the plateau of otherwise total external reflection. In a simplistic argument valid for infinite samples and beams, photons get trapped under the resonance conditions in the guiding layer propagating over an active coupling length (in our case $\sim$500–1000 μm) parallel to the surface, and are therefore more likely to get absorbed.[15] The enhanced absorption loss manifests itself as a pronounced decrease in the reflectivity. From the width of the cusps, the angular acceptance of the mode can be roughly estimated. In case of a finite structure cut off at one side, photons trapped in the guiding layer may also exit at the side leading to a beam of nanometer dimension. This may happen, if the footprint of the beam is separated from the edge of the sample by

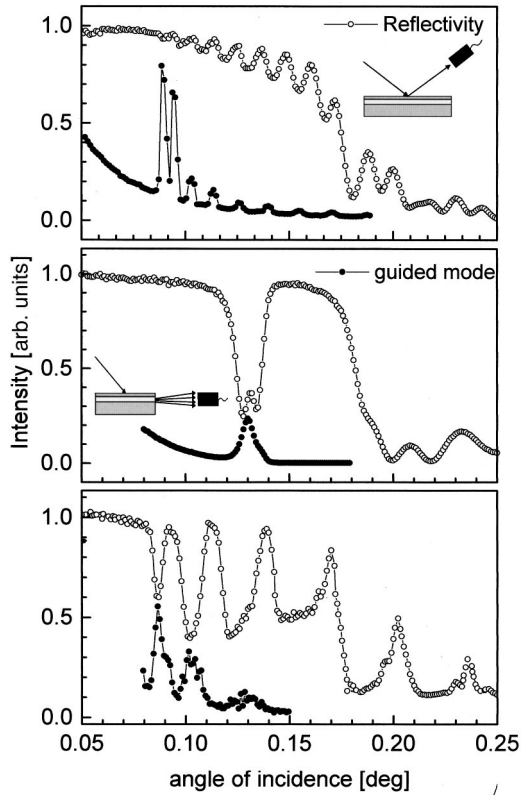

FIG. 3. Measured reflectivity (open circles connected by line) and waveguided mode (full circles connected by line) of a waveguide with a single 1098 Å carbon guiding layer (top), with two guiding layers (75 Å Ni/98 Å C/97 Å Ni/94 Å C/202 Å Ni/substrate) (middle) and with multiple guiding layers (7 $\times$[25 Å Ni/457 Å C]/200 Å Ni/substrate) (bottom) for 20 keV x rays.

not much further than the active coupling length.

Very clearly, the double and multiple guiding-layer structures give rise to a splitting and thus broadening of the cusps in the plateau of otherwise total external reflection, as expected from the simulations in Fig. 2. A more direct evidence of the waveguide effects and an assessment of its efficiency in the single and multiple guiding layer structures can be obtained by measuring the beam exiting horizontally from the sample, setting the detector to $\alpha_f=0$ with detector slits adjusted to integrate over $\pm 0.2°$ (corresponding to the divergence of the exiting mode). The corresponding curves as a function of α_i are shown together with the respective reflectivity curves, clearly demonstrating the enhanced angular acceptance compared to a single guiding-layer device. For the double (multiple) guiding layer device we estimate a fourfold (sevenfold) increase of the flux density compared to a hypothetical slit of the same cross section [which corresponds to a gain of 4(7) at that wavelength].[16]

To study the complete farfield pattern of the modes, we have measured the detected intensity both for the double and multiple guiding layer waveguide as a function of α_i and α_f. For the double guiding layer waveguide the results are shown in Fig. 4 in the form of two detector scans for angles of incidence $\alpha_{i,\mathrm{TE00}}=0.129°$ and $\alpha_{i,\mathrm{TE01}}=0.136°$ corresponding the two submodes of the TE0 mode. Apart from the peaks of the primary beam passing the sample at $\alpha_f=\alpha_i$ and the specular reflected beam at $\alpha_f=\alpha_i$ on can clearly see the

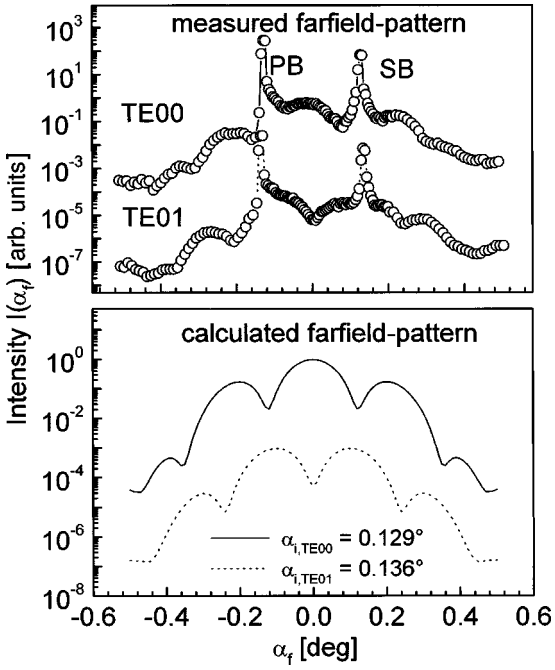

FIG. 4. Top: Measured farfield pattern $I(\alpha_f)$ of the excited TE00 and TE01 submode of a waveguide with two guiding layers (95 Å Ni/98 Å C/101 Å Ni/100 Å C/202 Å Ni/substrate). Bottom: Calculated farfield intensity distribution $I(\alpha_f)$ for the same structure for two angles of incidence corresponding to the TE00 and TE01 (20 keV x rays).

pronounced farfield interference reflecting the particular shape of the waveguided mode. The interference pattern is spread out over a wide angular range (particularly far into the area $\alpha_f<0$, where the sample shadows the direct beam). In the case of the multiple guiding layer device the data are represented as a logarithmically coded contour plot in Fig. 5. In this representation, the primary beam passing the sample at $2\theta=0$ appears as a straight vertical streak, the specular beam at $2\theta=2\alpha_i$ ($\alpha_i=\alpha_f$) as a straight but inclined streak. For the double (multiple) guiding layer waveguide an average width (FWHM in vertical direction) of the interference maxima of $\sim 0.004°$ ($\sim 0.03°$) and a periodicity $\Delta\alpha_{f,\max}^{\mathrm{measured}}$

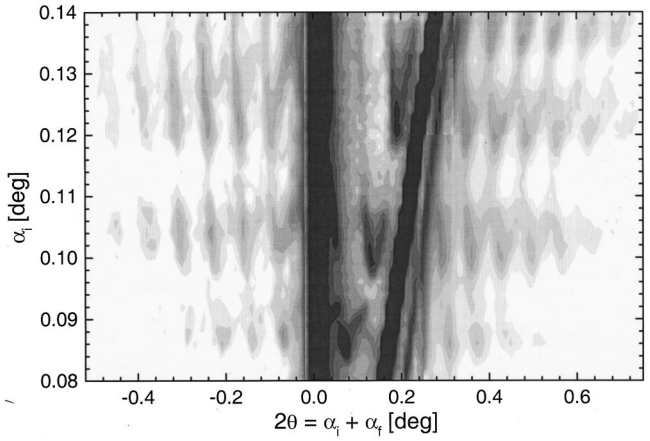

FIG. 5. Logarithmic contourplot of measured interference pattern as a function of α_i and $2\theta=\alpha_i+\alpha_f$ of a multiple guiding layer waveguide (7$\times$[25 Å Ni/457 Å C]/200 Å Ni/substrate) for 20 keV x rays.

$=0.207°$ ($\Delta\alpha_{f,\max}^{\text{measured}}=0.0727°$) at $\alpha_i=0.136°$ ($\alpha_i=0.105°$) was determined.

As a first approach for the explanation of the results we can consider the end of the waveguide as a grating with a spacing of 193 Å (482 Å) [the periodicity of the double (multiple) guiding layer stack $d=d_1+d_2$]. Illuminating the grating with a plane wave would result in a diffracted interference pattern with maxima at $d\sin\alpha_{f,\max}=\pm m\lambda$, where m is a positive integer and $d=d_1+d_2$. Evaluating the expression for the parameters of the multiple guiding layer waveguide one gets $\Delta\alpha_{f,\max}^{\text{theoretical}}=0.0736°$, which is in good agreement with the measured values. For the double layer waveguide the expected theoretical value $\Delta\alpha_{f,\max}^{\text{theoretical}}=0.184°$ is slightly smaller than the experimental value $\Delta\alpha_{f,\max}^{\text{measured}}=0.207°$. Although this is of course a very simple approach, we can understand the basic origin of the measured intensity distribution as a simple interference of the coherent beams exiting horizontally from the waveguide structure. For a more complete description of the phenomena, we have calculated farfield patterns for several excited submodes of the multiple guiding layer waveguide. In principle, this can be done in the same way as for waveguides with only one guiding layer, where the Fraunhofer farfield intensity distribution as a function of the exiting angle α_f (Ref. 17) is given in the approximation of small angles by

$$\mathcal{I}(\alpha_f)=\mathcal{I}_0\left|\int_{-\infty}^{+\infty}E_y(z)e^{ik_0\sin(\alpha_f)z}dz\right|^2. \tag{1}$$

Calculating the farfield pattern for two angles of incidence corresponding to the two submodes of the double guiding layer device results in the plots shown in Fig. 4 (bottom). The periodicity of the maxima in α_f has for both cases roughly the same value and compares well with the simple grating approach. However, the positions of the maxima are shifted against each other due to the different phase pattern of the two nearfields. While we see a maximum exactly centered at $\alpha_f=0°$ for $\alpha_i=0.129°$ (TE00), the farfield pattern calculated for $\alpha_i=0.136°$ shows two symmetric maxima at $\alpha_f=\pm 0.1°$. In the case of the multiple guiding layer device the farfield pattern is calculated for two angles of incidence corresponding to the lower ($\alpha_i=0.085°$) and upper ($\alpha_i=0.089°$) end of the TE0 band and shown in Fig. 6. Again we get a pattern with a centered maximum ($\alpha_i=0.085°$) and one with two symmetric maxima around $2\theta=\alpha_i$ ($\alpha_f=0$), but this time with a rather strong decay towards greater $|\alpha_f|$. Due to the different relative intensity decays, the farfield pattern with the single centered maxima is far more dominant in Fig. 5 than the other. Importantly, the simulation can clearly reproduce the experimental feature of the split, V-like shaped maxima in Fig. 5. In principle, the complete mapping can be simulated by this approach, which is however numerically rather slow. However, the effect of mode mixing, as observed and characterized by Feng, Deckmann, and Sinha in Ref. 18 for single guiding layer waveguides, should be expected to be more prominent in the present multiple guiding layer structures and may necessitate further modifications in the description.[8]

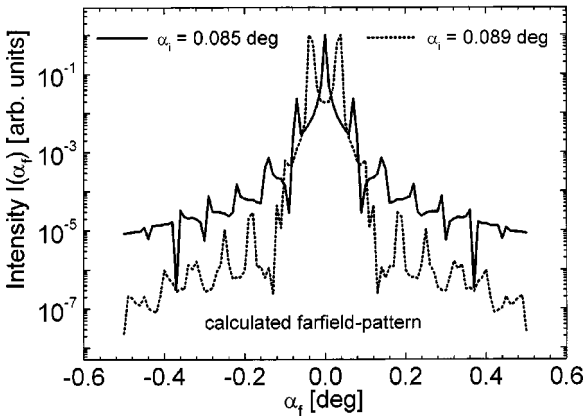

FIG. 6. Calculated farfield intensity distribution $I(\alpha_f)$ for two angles of incidence corresponding to the upper (dashed) and lower (line) end of the TE0-guiding band (20 keV x rays).

In summary, we have successfully demonstrated the principle of multiple guiding layer x-ray waveguide structures and have shown that they can be understood by a straightforward generalization of the single waveguide case. The results can most simply be understood as a grating structure for hard x rays with a tailored periodicity in the range $100\leqslant d\leqslant 2000$ Å, controlled by the design and growth of the structure. Importantly the device differs from a hypothetical transmission grating in that the field intensity impinging on the grating is enhanced up to two orders of magnitude by the waveguide resonance. Furthermore, one should be able to tailor specific shapes of the exiting coherent x-ray beam after careful parameter studies in the simulation of the electric field and the corresponding farfield, possibly leading to new focusing devices. Such optical components could be of particular interest for thermal and cold neutrons, where one could use structures with more than 100 resonance layers without significant limits by absorbtion. Guiding layer structures for hard x rays, e.g., with two guiding layers could lead to novel applications in x-ray interferometry, as the farfield distribution is crucially sensitive to phase changes in one of the interference beams. In this way information on the local, nanoscale electronic density can be projected onto macroscopic area detectors. Furthermore dynamic properties could also be probed in a two-beam or multibeam interference setup, as the exiting beam is fully coherent and therefore amenable to photon correlation spectroscopy.

We thank K. Ben-Saidane, W. Graf, and F. Berberich for their technical support and B. Toperverg, A. Frank, and D. Windt for a series of fruitful discussions.

[1] A. Malik *et al.*, Phys. Rev. Lett. **81**, 5832 (1998).
[2] S. Mochrie *et al.*, Phys. Rev. Lett. **78**, 1275 (1997).
[3] M. J. Zwanenburg *et al.*, Phys. Rev. Lett. **82**, 1696 (1999).
[4] C. Raven *et al.*, Appl. Phys. Lett. **23**, 1826 (1996).
[5] S. Kuznetsov *et al.*, Appl. Phys. Lett. **65**, 827 (1994).
[6] Y. P. Feng *et al.*, Phys. Rev. Lett. **71**, 537 (1993).
[7] S. Lagomarsino *et al.*, Appl. Phys. Lett. **71**, 18 (1997).
[8] F. Pfeiffer, T. Salditt, P. Høghøj, and I. Anderson (unpublished).
[9] F. Pfeiffer, Diploma thesis, Ludwig-Maximilians-Universität München, Sektion Physik, 1999.

[10] S. I. Zheludeva *et al.*, Crystallogr. Rep. **40**, 132 (1995).
[11] The coupling efficiency can best be characterized by comparing the flux exiting the waveguide (directly measurable by properly integrating over the farfield pattern) with the flux, which one would get using a hypothetical slit of the same cross section as dimension of the guiding layer. In the literature this ratio is also defined as the gain of the waveguide (see also Refs. 6 and 7).
[12] M. R. Shenon, K. Thyagarajan, and A. K. Gatah, J. Lightwave, J. Lightwave Technol. **LT-6**, 1285 (1988).
[13] L. G. Parratt, Phys. Rev. **95**, 359 (1954).
[14] The refraction index for x rays is given as $n=1-\delta-i\beta$, where δ is proportional to the electron density of the corresponding material. See also Ref. 11.
[15] P. K. Tien and R. Ulrich, J. Opt. Soc. Am. **60**, 1325 (1970).
[16] A somewhat less monochromatic would result in an even higher flux enhancement.
[17] In this formula the angle α_f should of course be measured between the detector and the horizon of the sample at the exit of the sample rather than the sample center.
[18] Y. P. Feng, H. W. Deckmann, and S. K. Sinha, Appl. Phys. Lett. **64**, 1 (1993).